Blind Correction of Gain and Timing Mismatches for a Two-Channel Time-Interleaved Analog-to-Digital Converter: Experimental Verification

Munkyo Seo, Mark J. W. Rodwell, and Upamanyu Madhow
Department of Electrical and Computer Engineering,
University of California, Santa Barbara, CA 93106 USA
Email: {mkseo, rodwell, madhow}@ece.ucsb.edu

***Abstract*—We report experimental verification of the previously proposed blind method of correcting gain and timing mismatches for a two-channel time-interleaved analog-to-digital converter (TIADC). The experimental setup allows for two different M=2 TIADC configurations with 14-bit resolution and 200-MHz overall sampling rates. Mismatch parameters are estimated by the blind algorithm with representative narrowband and wideband signals. The spurious-free dynamic range (SFDR) performance is then evaluated by using sinusoids. We discuss performance gain, as well as the limitations of the proposed blind algorithm when applied to real world analog-to-digital (A/D) converters.**

I. Introduction

A time-interleaved analog-to-digital converter (TIADC) has a parallel structure where a number of sub-converters cyclically sample the input signal, and outputs are similarly taken to form a digital stream. The overall sampling rate linearly increases with the number of sub-converters, therefore a TIADC is well suited for high-speed analog-to-digital (A/D) conversion systems [1], [2].

The spectral performance of a TIADC is limited by mismatches in electrical characteristics between sub-converters. In practice, gain, sampling time and dc offset mismatches are usually dominant. Such mismatches create noise sidebands, decreasing signal-to-noise ratio and spurious-free dynamic range (SFDR) [1], [7]. Post-correction of mismatch errors by digital signal processing provides two options: training methods [7] and blind methods [3]-[6], [8]. Training methods are capable of correcting general linear mismatches, and therefore are suitable for high-resolution applications at the cost of special calibration hardware and system stoppage. Blind methods, on the other hand, allow continuous system operation and track slowly time-varying mismatches, with limitations such as compromised accuracy and potentially high computational cost.

The authors have proposed a novel blind correction algorithm for gain and timing mismatches [8], which is more general than previous techniques, since, other than the input wide-sense stationarity (WSS) assumption, no special input distribution or sub-Nyquist bandwidth limitations are assumed. Gain and timing mismatches are handled in a unified framework of a parameterized filter bank. Uniqueness proof of the estimate was also given for the first time. This paper is an experimental continuation of the authors' prior work toward making blind mismatch correction more practical.

II. Review of The Proposed Blind Correction Algorithm

This section summarizes the previously proposed blind method [8]. A two-channel TIADC system is shown in Fig.1 (a), where the analog input $x(t)$ is assumed to satisfy Nyquist sampling criterion. The gain and timing mismatches for the first and second channel are $(G_0, \Delta t_0)$ and $(G_1, \Delta t_1)$, respectively. Fig.1 (b) is a channel-transfer-function (CTF) representation where $H_i(\omega)=G_i\exp(-j\omega\Delta t_i)$. As shown by experimental data later, actual sample-and-hold circuits and A/D converters exhibit general linear gain-phase distortion as well as static gain and timing delay, which can be appropriately modeled by CTF's. Normalization with respect to $H_0(\omega)$ yields Fig.1 (c), which leaves only two relevant mismatch parameters, $G \equiv G_1/G_0$, and $\Delta t \equiv \Delta t_1 - \Delta t_0$ in the static gain and timing model. This normalization disregards linear filtering common to both channels, and serves as a logical starting point for blind correction.

Assume $x(t)$ has WSS property. Then, its autocorrelation $R_x(t_2,t_1)\equiv E[x(t_2)x(t_1)]$ is shift-independent and depends only on the time lag such that $R_x(t_2,t_1)=R_x(t_2-t_1)$. If $(G, \Delta t)=(1,0)$, i.e. no mismatch, then $y[n]=x(nT_s)$ (disregarding common filtering) will also exhibit WSS property such that its autocorrelation $R_y[n,m]\equiv E[y[n]y[m]]$ is shift-independent. If $(G, \Delta t)\neq(1,0)$, however, WSS property will be lost, and $y[n]$ will exhibit wide-sense cyclo-stationarity (WSCS). $R_y[n,m]$ will be then periodic with respect to shift, such that $R_y[n,m]=R_y[n+2,m+2]$ and $R_y[n,m] \neq R_y[n+1,m+1]$ in general.

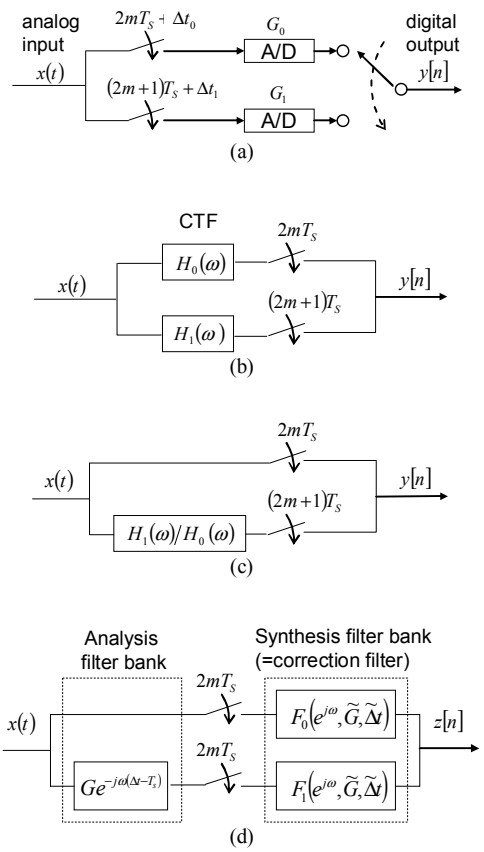

Figure 1. A M=2 TIADC system: (a) actual system, (b) general CTF representation, (c) after normalization, and (d) with correction filters.

Now, we cascade a correction filter, and the resulting system can be represented as a standard analysis-synthesis filter bank form in Fig.1 (d) [8]-[9]. The correction filter is parameterized by mismatch estimates $(\tilde{G}, \tilde{\Delta t})$ such that perfect reconstruction condition is met when the estimation is equal to the true ones, i.e., when $(\tilde{G}, \tilde{\Delta t}) = (G, \Delta t)$ [8]. Let $z[n]$ and $R_z[n,m]$ be the synthesis filter bank output and its autocorrelation, respectively. We want to restore WSS property by adjusting $(\tilde{G}, \tilde{\Delta t})$. The following error measure quantifies how $z[n]$ is close to being WSS.

$$J(\tilde{G}, \Delta\tilde{t}) \equiv \sum_{u=0}^{U_{\max}} \left(R_z[0,u] - R_z[1,1+u]\right)^2 \qquad (1)$$

When $z[n]$ is perfectly WSS, J is identically zero, and the estimate is guaranteed to be equal to true parameters [8]. In practice, we iteratively adjust the estimation $(\tilde{G}, \tilde{\Delta t})$ to reach the minimum of J. In summary, we first empirically obtain $R_y[0,u]$ and $R_y[1,1+u]$ by observing the uncorrected TIADC output. Second, given the current parameter estimate, the correction filter is designed from perfect reconstruction condition [8]. Third, $R_z[0,u]$ and $R_z[1,1+u]$ is calculated from $R_y[n,m]$ by applying double convolution with a correction filter. Finally, adjust $(\tilde{G}, \tilde{\Delta t})$ until finding the minimum of J defined in (1).

III. Experimental Result

A. System Setup and Input Signal Preparation

The experimental setup is similar to the previous one [7], except for an arbitrary waveform generator (AWG520 from Sony/Tektronix) to create wideband signals. Clock and input signals are fed to four A/D boards (AD6645 from Analog Devices, Inc.), each having 14-bit resolution and 100-Msamples/S (MSPS) of sampling rate. A logic analyzer captures the digital output, and correction is done on MATLAB™. The setup operates at 200-MSPS as a two-channel TIADC by choosing either 1st- and 3rd-, or 2nd- and 4th-channel, which will be referred to as "TIADC-13" and "TIADC-24," respectively.

Two kinds of input signals are considered for the purpose of blind estimation: (a) sinusoids from 1.6 to 99.2-MHz in 1.6-MHz step, and (b) 80-MHz bandwidth signal randomly colored by 10-tap FIR filters, as representative narrowband and wideband signals, respectively. Wideband signals are prepared by first generating uncorrelated sequence of uniform-distributed samples, filtering sharply to define occupied bandwidth, and randomly coloring.

B. Algorithm Implementation and Performance Evaluation

Optimization of the error measure in (1) is done by calling a MATLAB built-in function, *fminsearch*, with all available data samples, rather than in adaptation with incremental samples [4]-[6]. This allows us to look at more fundamental behaviors without artifacts due to the adaptation. No local minimum was observed throughout optimization runs. Important parameters are L (=71), the number of correction filter taps, N_{sample} ($=3 \cdot 10^4$ for sinusoids, and 10^6 otherwise), observation sample size, and U_{max} (=10), autocorrelation window in (1). Default values are shown in the parenthesis.

For experimental study, comparing SFDR before and after blind correction is more practical performance evaluation than comparing the estimation of mismatch parameters with true ones, as in earlier simulation study [8]. *Regardless of the input signal type for mismatch estimation, SFDR evaluation is performed using only sinusoidal signals* due to the desirable frequency localization and high dynamic range property. Offset spur is not considered in measuring SFDR. For sinusoidal tests, harmonics up to 8th-order (<-40dBc), from the signal generator, are also ignored.

C. Measured Channel-Transfer-Function

Fig. 2 shows normalized CTF's, characterized by a training method [7], for TIADC-13 and TIADC-24. It is seen that, except at low frequencies below 20-MHz, the CTF can be approximately described by a static gain time delay model, $(G, \Delta t)$, which is roughly $(1.002, 0.005T_s)$, and $(0.99, 0.002T_s)$ for TIADC-13 and TIADC-24, respectively. The large deviation below 20-MHz is due to the cut-off mismatches of input transformers on A/D boards. Full

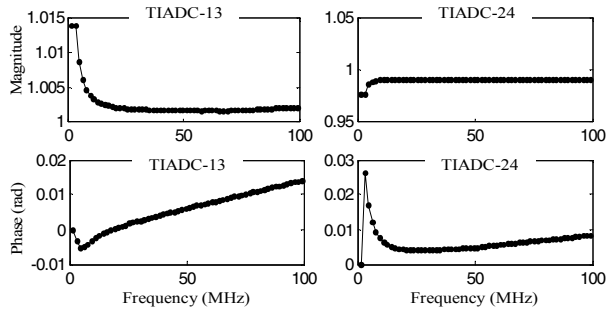

Figure 2. Normalized CTF's for TIADC-13 (left) and TIADC-24 (right).

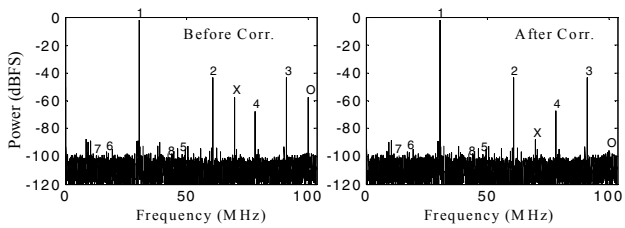

Figure 3. Typical output spectrum before (left), and after (right) blind correction with an input sinusoid at 30.4MHz. The gain and timing mismatch spurs are marked as 'X', and offset spur as 'O'. Harmonics from signal generators also shown as numbers.

correction of these frequency-dependent mismatches will require training methods [7].

D. Blind Correction With Sinusoidal Inputs

A series of data acquisition is performed with sinusoidal inputs varying its frequency from 1.6-MHz to 99.2-MHz with 1.6-MHz step. As a first test, three sets of correction filter coefficients are obtained by the proposed blind method with the input sinusoid at 4.8, 38.4, and 76.8-MHz. SFDR performance is then evaluated across the full Nyquist zone for each correction filter. Fig.3 shows typical output spectrum, and Fig.4 summarizes SFDR performance for each correction filter.

It is seen that the improvement in SFDR is at its peak (20~40dB) around the calibration frequencies, but is decreasing as the frequency moves away. In particular, the correction filter obtained with 4.8MHz input provides ~20 dB gain at the calibration center (the solid line with leftmost peak in both plots in Fig. 4), but the SFDR quickly drops below the uncorrected one as we go away from the correction frequency. We note here two important properties of the blind correction algorithm. First, the blind algorithm only "sees" the CTF at those frequencies where the TIADC input has nonzero power. In other words, the TIADC output does not have any information about the unexcited mode of the A/D converter frequency response. Second, the blind algorithm seeks to find the best estimate $(\tilde{G}, \tilde{\Delta t})$ which can compensate for the excited mode of the actual CTF. Assume a single-tone input at ω_0, and the CTF at this frequency H(j ω_0). Then, the blind algorithm

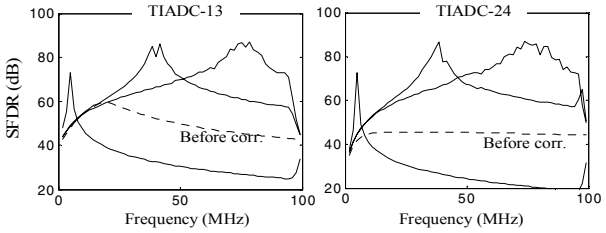

Figure 4. Blind correction result with sinusoidal inputs for TIADC-13 (left) and TIADC-24 (right). Dotted lines represent uncorrected SFDR, and solid lines corrected SFDR with filters obtained from 4.8, 38.4, and 76.8 MHz input, where the SFDR peak corresponds to the input frequency.

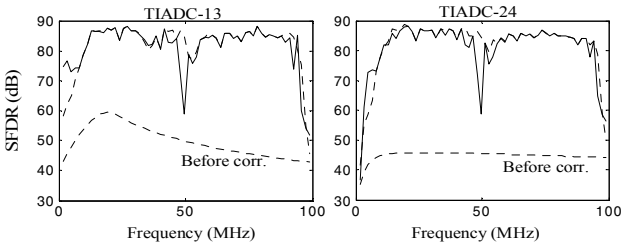

Figure 5. Blind correction result with sinusoidal inputs. Correction filters are re-calculated at every SFDR evaluation frequency.

concludes parameter search with the equivalent gain and time delay as follows.

$$G_{eq} = |H(j\omega_0)|, \ \Delta t_{eq} = \frac{\angle H(j\omega_0)}{\omega_0} \qquad (2)$$

If the actual CTF is exactly represented by static gain and time delay over the entire Nyquist zone, then the estimation (2) will provide full-band correction. If, however, the CTF deviates from (G, Δt) model, then (2) will provide only narrowband mismatch correction at ω_0, and at other frequencies, the mismatch may or may not be corrected. In Fig. 2, it is seen that the behavior of CTF at 4.8 MHz is not consistent with (G, Δt) model. The mismatch parameters estimated at this frequency, therefore, do not accurately model the overall frequency-domain behavior, thus failing in providing wideband correction as seen in Fig. 4.

As a second narrowband test, noting that the correction is still locally valid around the calibration frequency, we now recalculate the correction filter for every SFDR evaluation frequency, and the result is shown in Fig. 5. For reference, off-line calibration result [7] is also shown as a dotted-line, which overlaps over substantial frequency regions. In both cases, mismatch spurs are suppressed enough so that SFDR is mostly limited by other spurs unrelated to channel mismatches, thus the similar SFDR results between the off-line and blind method (In an off-line method, however, the full-band correction is achieved by a single set of filter coefficients). In Fig. 5, sudden SFDR drop around 50-MHz is due to the artificial, unreal mismatch induced by the input signal, not actual channel mismatches. A single period of a 50-MHz sinusoid is exactly equal to $4T_s$, such that in the worst case, the first and second A/D converter may only

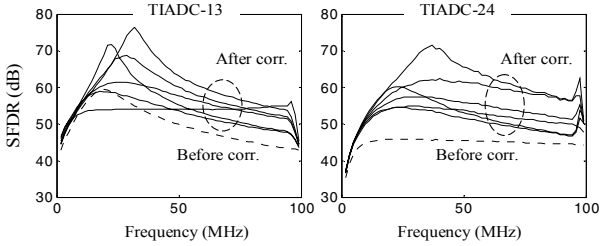

Figure 6. Blind correction result with six dc-to-80-MHz wideband inputs.

catch peaks and zero-crossings, or vice versa, of a sinusoid, respectively. This signal-induced mismatch is indistinguishable from actual channel mismatches with the present method. Put in another way, input WSS assumption is not valid in this case and we need either much longer observation or randomization techniques.

Fig. 4 and 5 are representative demonstrations of the blind method assuming narrowband WSS signals. In reality, the center frequency of the input may be time-varying and the correction filter will also be updated at a certain rate. Fig. 4 shows the expected SFDR performance after a sudden change in input frequency before filter coefficients are updated. Fig. 5, on the other hand, exemplifies the opposite scenario where the input frequency changes more slowly than the coefficient update rate.

E. Blind Correction With 80-MHz Bandwidth Signals

Six 80-MHz bandwidth signals are applied for the purpose of mismatch estimation. The SFDR performance is evaluated by using sinusoids and summarized in Fig. 6. The blind algorithm now "sees" the CTF over a wider range of frequencies than the narroband input case, and therefore the estimated parameters provide a better fit to the entire frequency response. The SFDR improvement is more evenly distributed, but still depends on the input power distribution. For example, one of the test inputs happens to have ~15dB higher power level around 50-MHz. When applied to TIADC13, its corrected SFDR is seen to be lower than the uncorrected one, below 30-MHz.

F. The Effects of Observation Sample Size

The estimation error of the proposed blind method is critically related to the autocorrelation estimation accuracy as seen in (1). Assuming a WSS source, it can be shown that the variance of non-WSS noise of autocorrelation estimation, due to the finite observation, is inversely proportional to N_{sample}^2 and N_{sample}, for asymptotically narrowband and wideband signals, respectively. Further analysis is beyond the scope of this paper and instead we summarize representative experimental results in Fig. 7.

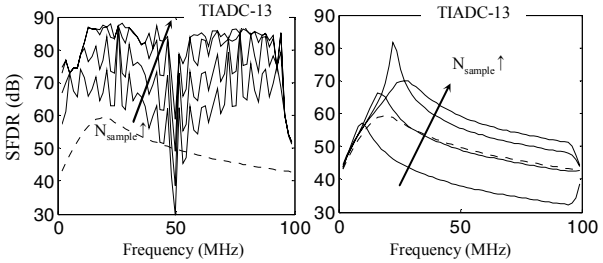

Figure 7. The effects of observation sample size (TIADC-13): (a) sinusoidal inputs with self-obtained correction filters at every SFDR evaluation frequency. $N_{sample}=10^3$, $3\cdot10^3$, 10^4, and $3\cdot10^4$. (b) 80-MHz bandwidth input with $N_{sample}=3\cdot10^4$, 10^5, $3\cdot10^5$, and 10^6.

IV. CONCLUSION

We have discussed experimental verification of the blind method for TIADC mismatch correction. Under the present experimental condition, mismatch modeling error is limiting broadband correction. The finite observation sample size also limits the SFDR performance with wideband signals. Further studies are currently under way to achieve a more satisfactory broadband correction. Modification of the current algorithm for real-time operation will also be explored.

REFERENCES

[1] W. C. Black, Jr. and D. A. Hodges, "Time interleaved converter arrays," *IEEE J. Solid-State Circuits*, vol. SC-15, no. 6, pp. 1022-1029, Dec. 1980.

[2] K. Poulton, R. Neff, B. Setterberg, B. Wuppermann, T. Kopley, R. Jewett, J. Pernillo, C. Tan, and A. Montijo, "A 20GS/s 8b ADC with a 1MB memory in 0.18um CMOS," *ISSCC Dig. Tech. Paper*, pp. 318-319, 2003.

[3] S. M. Jamal, D. Fu, M. P. Singh, P. J. Hurst, and S. H. Lewis, "Calibration of sample-time error in a two-channel time-interleaved analog-to-digital converter," *IEEE Trans. Circuits and Systems-I: Regular papers*, vol. 51, no. 1, pp. 130-139, Jan. 2004.

[4] V. Divi and G. Wornell, "Signal recovery in time-interleaved analog-to-digital converters," in *Proc. IEEE ICASSP*, vol. 2, pp. 593-596, May 2004.

[5] J. Elbornsson, F. Gustafsson, and J.-E. Eklund, "Blind adaptive equalization of mismatch errors in a time-interleaved A/D converter system," *IEEE Trans. Circuits and Systems – I: Regular Papers*, vol. 51, No. 1, pp. 151-158, Jan. 2004.

[6] J. Elbornsson, F. Gustafsson, and J.-E. Eklund, "Blind equalization of time errors in a time-interleaved ADC system," *IEEE Trans. Signal Processing*, vol. 53, no. 4, pp. 1413-1424, Apr. 2005.

[7] M. Seo, M. Rodwell, and U. Madhow, "Comprehensive digital correction of mismatch errors for a 400-MSamples/S, 80-dB SFDR time-interleaved analog-to-digital converter," *IEEE Trans. Microwave Theory Tech.*, vol. 53, no. 3, pp. 1072-1082, Mar. 2005.

[8] M. Seo, M. Rodwell, and U. Madhow, "Blind correction of gain and timing mismatches for a two-channel time-interleaved analog-to-digital converter," *39th Asilomar Conference on Signals, Systems, and Computers*, October 2005.

[9] P. P. Vaidyanathan, *Multirate Systems and Filter Banks*, Englewood Cliffs, NJ: Prentice-Hall, 1993